International Journal of Cardiology 275 (2019) 136–144

Contents lists available at ScienceDirect

International Journal of Cardiology

journal homepage: www.elsevier.com/locate/ijcard

Stem cells transplantation positively modulates the heart-kidney cross talk in cardiorenal syndrome type II

Giorgio Vescovo [a], Chiara Castellani [b], Marny Fedrigo [b], Grazia Maria Virzì [c,d], Giovanni Maria Vescovo [b], Regina Tavano [e], Michela Pozzobon [f,g], Annalisa Angelini [b,*]

[a] Internal Medicine, S. Antonio Hospital, Italy
[b] Dept. Cardiac Thoracic, Vascular Sciences and Public Health, University of Padua, Italy
[c] Department of Nephrology, Dialysis and Transplant, San Bortolo Hospital, Vicenza, Italy
[d] IRRIV-International Renal Research Institute Vicenza, San Bortolo Hospital, Vicenza, Italy
[e] Dept. Biomedical Sciences, University of Padua, Italy
[f] Dept. Women and Children Health, University of Padua, Italy
[g] Insitute of Pediatric Research Città della Speranza, Padova, Italy

ARTICLE INFO

Article history:
Received 31 July 2018
Received in revised form 4 October 2018
Accepted 9 October 2018
Available online 16 October 2018

Keywords:
Cardiorenal syndrome type II
NGAL
Stem cells
Congestive heart failure
Remodeling

ABSTRACT

Introduction: We investigated the effects of human amniotic fluid stem cells (hAFS) and rat adipose tissue stromal vascular fraction GFP-positive cells (rSVC-GFP) in a model of cardio-renal syndrome type II (CRSII).
Methods and results: RHF was induced by monocrotaline (MCT) in 28 Sprague-Dawley rats. Three weeks later, four million hAFS or rSVC-GFP cells were injected via tail vein. BNP, sCreatinine, kidney and heart NGAL and MMP9, sCytokines, kidney and heart apoptosis and cells (Cs) engraftment were evaluated.
Cell-treated rats showed a significant reduction of serum NGAL and Creatinine compared to CRSII. In both hAFS and rSVC-GFP group, kidney protein expression of NGAL was significantly lower than in CRSII (hAFS $p = 0.036$ and rSVC-GFP $p < 0.0001$) and similar to that of controls. In both hAFS and rSVC-GFP treated rats, we observed cell engraftment in the medulla and differentiation into tubular, endothelial and SMCs cells. Apoptosis was significantly decreased in cell-treated rats (hAFS 14.07 ± 1.38 and rSVC-GFP 12.67 ± 2.96 cells/mm^2) and similar to controls (9.85 ± 2.1 cell/mm^2). TUNEL-positive cells were mainly located in the kidney medulla. Pro-inflammatory cytokines were down regulated in cell-treated groups and similar to controls. In cell-treated rats, kidney and heart tissue NGAL was not complexed with MMP9 as in CRSII group, suggesting inhibition of MMPs activity.
Conclusion: Cell therapy produced improvement in kidney function in rats with CRSII. This was the result of interstitial, vessel and tubular cell engraftment leading to tubular and vessel regeneration, decreased tubular cells apoptosis and mitigated pro-inflammatory milieu. Reduction of NGLA-MMP9 complexes mainly due to decrease MMPs activity prevented further negative heart remodeling.

1. Introduction

Cariorenal syndrome type II (CRSII) is defined as kidney injury in the setting of chronic heart failure [1,2]. Many are the mechanisms underlying kidney damage. These encompass decrease cardiac output with low kidney perfusion inducing reduced glomerular function, splanchnic congestion leading to tubular injury, neuroendocrine and inflammatory factors [1,2]. In CRSII the heart-kidney crosstalk is as such that kidney damage, once established, produces a vicious circle that in turn leads to a further heart damage [3,4,5]. The reversibility of kidney damage in CRSII is still debated. Neither in animal studies, nor in heart failure clinical trials, this hypothesis has been ever demonstrated. One possible future development is the use of stem cells to ameliorate kidney function by acting on paracrine mechanisms, decreasing inflammation, repairing tissue damage and producing organ favorable remodeling [6–8]. These hypotheses have been confirmed in diabetic nephropathy [9–11] and in models of kidney damage where mesenchymal bone marrow stem cells [12–16] and human adipose derived stem cells were used [17].

Aim of our study was to explore whether in an animal model of right congestive heart failure (the monocrotaline treated rat), the in-vivo administration of adipose stromal vascular cells or amniotic fluid stem cells was able to block and/or reverse the pathophysiological mechanisms leading to congestion-induced tubular damage in CRSII.

* Corresponding author at: Dept. of Cardiac, Thoracic, Vascular Sciences and Public Health University of Padova, Via A. Gabelli, 61, 35128 Padova, Italy.
E-mail address: annalisa.angelini@unipd.it (A. Angelini).

https://doi.org/10.1016/j.ijcard.2018.10.038
0167-5273/

2. Material and methods

2.1. Animals and experimental protocols and cells characterization

2.1.1. Animals and experimental protocols

Right sided heart failure (RHF) was induced in male Sprague-Dowley rats, weighting 90 to 100 g, by injecting intraperitoneally 30 mg/Kg of monocrotaline (MCT) according to Vescovo et al. [18–26].

MCT is a well-established model of RHF which mimics the CHF syndrome in man [17–26].

After 21 days, a time-point when pulmonary hypertension (PH) is present and right ventricle (RV) hypertrophy and right ventricle failure (RVF) have developed, the rats were randomly separated into three different groups:

I. Ten MCT rats treated with saline, serving as a control group with PH and RVF (CRSII group)
II. Seven CRSII rats injected with c-Kit–selected hAFS harvested from human amniocentesis specimens (hAFS group)
III. Eleven CRSII rats injected with rSVC-GFP, stromal vascular fraction cells harvested from adipose tissue of GFP rats (rSVC-GFP group).

Another group of ten rats treated with saline served as control group.

All the groups received treatment with cyclosporine (10 mg/kg/die) and azitromycin in drinking water, which was started at day 21 after MCT administration.

All animals were killed at day thirty. Hearts and Kidney were excised and frozen in liquid nitrogen or paraformaldehyde-fixed and paraffin-embedded. Blood samples were also collected.

Experiments were approved by the University of Padua Biological Ethical Committee and the Investigation conforms to the Guide for Care and Use of Laboratory Animals published in 1996 by the US National Institute of Health [6,7].

2.1.2. Isolation, culture and injection of hAFS cells

Human AFS c-Kit selected (hAFS) cells were derived according to De Coppi et al. [28], and Angelini et al. [6,7]. Samples of amniotic fluid cells (AF) were collected by amniocentesis mean gestational age 12 weeks, during routine prenatal diagnosis. A written consensus was obtained from each woman to use the AF experimentally.

Cytogenetic analysis was performed as reported in Angelini et al. and Castellani et al. [6,7]. These cells showed self-renewal and multi-lineage potential as already described [27–28].

Characterization of hAFS has been already performed and previously reported [7,28].

During all culture periods (from P3 to P8), hAFS cells highly expressed (90%) CD29, CD44 (hyaluronate receptor) and stromal cell markers as CD90 (Thy-1), CD105 (endoglin, TGFbeta receptor) and CD73. Cells also expressed HLA-ABC but not HLA-DR. The absence of the latter and the CD73 detection indicate low immunogenicity profile of the selected and cultured cells [6,7,28].

2.1.3. Cytofluorimetric analysis of hAFS cells

Human AFS cells were incubated with anti-human antibodies: CD29 FITC, CD44.

FITC, CD73 PE, CD90 FITC, CD105 PE, CD80 FITC and CD86 PE (Beckton Dickinson, Pharmingen, San Jose, CA), SSEA-4 FITC (Santa Cruz). Cells have been analyzed for HLA-ABC FITC and HLA-DR PE (Immunotech, Marseille, France).

Analysis was performed by a COULTER Epics XL-MCL cytometer (Beckman Coulter, CA) and data were elaborated by means of EXPO™ 32 ADC Software.

After 5–6 passages 4×10^6 cells were suspended in a Dulbecco solution and injected [6,7]. In a previous series of experiments we demonstrated the absence of effects of the Dulbecco solution injected in a group of normal rats [6,7].

2.1.4. Isolation, characterization and injection of rSVC-GFP cells

The stromal vascular fraction was isolated from subcutaneous adipose tissue of 3-months-old GFP+ transgenic Wistar rats upon collagenase type II digestion (1 mg/mL) (Sigma-Aldrich) in DMEM at 37 °C for at least 1 h. The sedimented stromal vascular cells (rSVC) obtained by 350*g* centrifugation were re-suspended in an erythrocyte-lysing buffer for 5 min and then washed two times in DMEM [6,7].

Freshly isolated rSVC-GFP expressed CD29, CD44 and CD73, even though a lower percentage of cells was positive compared to hAFS. The presence of these mesenchymal markers highlighted the stromal properties of the obtained cells. The positivity for CD31 and CD34 may be related to the vascular precursor component of this cell population.

Since the cells have not been selected, we could detect a low percentage of CD45 positive cells. For more details, refer to previously data published by our group [6,7].

rSVC-GFP cells includes a population of vascular cells (pericytes and endothelial progenitor cells), progenitor cells and multipotent mesenchymal cells [29–31].

2.1.5. Cytofluorimetric analysis of rSVC-GFP positive cells

Rat SVC-GFP positive cells were incubated with CD29-FITC, CD31-PE, Cd34-PE, CD44-FITC, CD45-PE, CD73-PE, purchased from BD and Biolegend.

Analysis was performed by a COULTER Epics XL-MCL cytometer (Beckman Coulter, CA) and data were elaborated by means of EXPO™ 32 ADC Software.

After characterization, freshly isolated 4×10^6 cells in 500 μL DMEM were suspended in a Dulbecco solution and immediately injected via tail vein in the recipient rats as described above [3].

2.1.6. Assessment of RV hypertrophy and failure

In order to make sure that the MCT animals developed RHF, beyond the well-known post-mortem signs such as pericardial, pleural and peritoneal effusions, the following measurements were taken:

- Right Ventricle Mass/Left Ventricle Mass (RVM/LVM) (Index of Hypertrophy)
- Right Ventricular Mass/Right Ventricular Volume index (RVM/RVV) (Index of dilatation) [6,7,18].

These two latter indices were calculated with a validated procedure currently adopted in our laboratory, using a computer-based image analyzer system consisting of an Olympus BH2 optical microscope connected to a computer via a video camera (JVC 3-CCD, Yokohama, Japan) and software for image analysis (Image PRO-Plus 4.0; Media Cybernetics, Silver Spring, MA), on formalin fixed transverse sections of the heart taken in the middle portion of the interventricular septum [6,7].

2.1.7. Assessment of cell death and kidney histology

In situ nick-end labeling (TUNEL) of fragmented DNA was performed on cryo-sections of the heart and kidney using an in situ cell death detection kit (POD; Boehringer Mannheim). Labeled nuclei were identified from the negative nuclei counterstained by DAB and counted after being photographed. The total number of positive nuclei was determined by counting (magnification 250×) all the labeled nuclei present in the entire specimen. The number of positive nuclei was then expressed as number of TUNEL-positive nuclei per square millimeter [3,6,7] Kidney Histology was performed on longitudinal sections of the entire left kidney of each animal. H&E and trichrome stains were used for detection of inflammation, congestion, glomerular and tubular damage.

2.2. Biomarker assessment of heart failure and CRSII occurrence

2.2.1. Brain natriuretic peptide assessment

Brain natriuretic peptide (BN) was measured on sera with an enzyme- linked immunoassay (ELISA kit; BNP-45 Cat. No. EK-011-17; Phoenix Pharmaceuticals, Inc., Burlingame, CA) following the manufacturer's instructions. The antibody was specific for rat BNP [3].

2.2.2. Creatinine assessment

Creatinine was measured on sera with an enzyme-linked immunoassay (Rat Creatinine (Cr) ELISA kit; CUSABIO BIOTECH CO., TEMA Ricerca, Italy) following the manufacturer's instructions. The antibody was specific for rat Creatinine. Values were expressed in pg/mL [3].

2.2.3. Neutrophil gelatinase-associated lipocalin (NGAL) assessment on sera

Neutrophil gelatinase-associated lipocalin (NGAL) was measured on sera with an enzyme-linked immunoassay (Rat NGAL ELISA kit; BIOPORTO Diagnostics, Bioexe Research Technology, Verona, Italy) following the manufacturer's instructions. The antibody was specific for rat NGAL [3].

2.2.4. Bio-Plex multiplex cytokine assays

2 mL whole blood was obtained from each rat; after 30′ incubation at 37 °C to induce coagulation, samples were centrifuged at 13200 rpm for 10 min at 4 °C. Serum samples were then analyzed through a Bioplex suspension array system (Bio-Rad, Milan, Italy) in order to quantify 9 cytokines: IL-1α, IL-1β, IL-2, IL-4, IL-6, IL-10, GM-CSF, IFN-γ and TNF-α, following the manufacturer's instructions. Briefly, serum samples and standards were incubated with a mixture of 5000 beads for cytokine for 30 min at room temperature in a 96-well sterile filter plate; after three washings, a cocktail of biotinylated antibodies was added; after a 30-minute incubation and three washings, streptavidin-PE was added to the samples. Finally, after a 10-minute incubation, the plate was read with Bioplex Manager software (Bio-Rad, Milan, Italy) [32].

2.3. Molecular tissue remodeling

2.3.1. Immunoblotting of NGAL and MMP9 proteins on heart and kidney tissues.

Heart and kidney samples were homogenized and solubilized in sodium dodecyl sulfate (SDS) buffer [6,32,33]. Protein quantification was performed using Qubit® Protein assay Kit (Life Technologies, Monza, Italy) according to the manufacturer's instructions. Protein samples were mixed with a non-reducing and reducing buffer and incubated for 5 min at either room temperature (reducing and non denaturating conditions) or 95oC (reducing and denaturating conditions).

All samples were subsequently separated on a 10% gel in a SDS-PAGE and transferred onto a nitrocellulose membrane (Amersham, Euroclone, Italy). The membrane was blocked for 1 h with 5% non-fat milk in the TBS containing 0.5% (v/v) Triton X-100.

(Sigma-Aldrich), and incubated overnight with polyclonal goat antibodies against MMP9, or NGAL (1:500, Abcam, Prodotti Gianni, Milan, Italy). Blots were developed using the SuperSignal West Femto ECL substrate (Pierce, Euroclone, Italy).

The percent distribution of the NGAL and MMP9 antibodies was determined by a densitometric software (Alliance 2.7 1D fully automated software) after image acquisition by Alliance 2.7 (UVITEC, Eppendorf, Italy) [3].

2.4. Transplanted cells engraftment and differentiation

2.4.1. Immunohistochemistry and double-immunofluorescence study

Kidneys paraffin-embedded sections (5 μm thick) were prepared, treated, and stained for immunohistochemistry according to standard procedures.

The antibodies used were GFP-specific antibody (Abcam, Prodotti Gianni, Milan, Italy), alfa human mitochondria antibody (Thermo Scientific, USA), alfa smooth muscle actin (DakoCytomation, Glostrup, Germany), alfa von Willebrand factor (Chemicon, Prodotti Gianni, Milan, Italy), CD68 (macrophages, Chemicon, Prodotti Gianni, Milan, Italy), anti MNF116 (Prodotti Gianni, Milan, Italy). Bound antibodies were visualized with anti-mouse or anti-rabbit FITC or rhodamine (TRITC)-conjugated secondary antibodies (Chemicon, Millipore, Prodotti Gianni, Milan, Italy). Nuclei were stained with TO-PRO-3 (Invitrogen, Molecular Probes, Eugene, OR). Micrographs were taken using a laser scanner confocal microscope (Model TCS-SL; Leica, Germany). Samples were also taken from spleen and rSVC-GFP and hAFS cells counted to exclude excessive hemocatheresis.

2.4.2. Assessment of cells differentiation

Similarly hAFS and rSVC-GFP co-expressing alfa SMA, vWf and positive cells were counted by two independent pathologists on high-power images. Three sections per animal and 12 randomly chosen fields per section were evaluated. Cells number was expressed either as percentage or total number per μm [2] [6,7].

2.5. Statistical analysis

Means ± SD or means ± SE were calculated. Student *t*-test for unpaired data and analysis of variance were used. A 5% difference was defined as statistically significant. ANOVA was used for comparing differences in cytokine levels.

3. Results

3.1. Evaluation of occurrence of heart failure and CRSII

3.1.1. Morphological data

At post-mortem examination, CRSII rats showed pericardial, pleural and peritoneal effusions characteristic of Heart Failure (HF). LVM/RVM, which is an index of RV hypertrophy, was significantly decreased in CRSII animals compared with controls (1.584 ± 0.156 vs 2.838 ± 0.354, $p < 0.0001$), indicating that RV developed hypertrophy (Fig. 1A). Stem cells treated rats (SCT) showed intermediate values between CRSII rats and controls for both hAFS (2.084 ± 0.200, $p < 0.0001$ vs CRSII) and rSVC-GFP groups (2.164 ± 0.274, $p = 0.012$ vs CRSII), indicating decreased RV hypertrophy after cell-treatment. RVM/RVV, an index of RV dilation, in SCRII rats was significantly lower compared to controls, indicating that, for a similar RV mass, there was a greater RV dilation (Fig. 1A). Both hAFS (2.184 ± 1.01, $p < 0.001$ vs CRSII) and rSVC-GFP (2.249 ± 0.723, $p = 0.03$ vs CRSII) showed higher values for RVM/RVV compared with CRSII group, suggesting that RV dilation was reduced. Clearly these values were not equal to those of controls, but they confirmed a trend toward a positive remodeling in terms of reduction of RV hypertrophy and dilatation.

3.1.2. Biomarkers of heart failure and CRSII

BNP was increased in CRSII rats when compared to controls (4.833 ± 1.329 ng/mL vs 1.427 ± 0.422 ng/mL, $p < 0.0001$). hAFS and rSVC-GFP rats groups showed a significant decrease when compared with CRSII (2.314 ± 0.793 ng/mL and 2.345 ± 1.025 ng/mL, $p = 0.0012$ and $p = 0.0038$ vs CRSII respectively, Fig. 1A).

The occurrence of kidney damage in CRSII rats was demonstrated by the significantly higher values of sCreatinine (3.5 ± 3.3 pg/mL, $p = 0.012$ vs controls) and sNGAL (532.7 ± 280 ng/mL, $p = 0.02$ vs controls) compared to controls (sCrea 0.5 ± 0.6 pg/mL and sNGAL 245.3 ± 154 ng/mL).

In hAFS and rSVC-GFP groups sCreatinine and sNGAL were reduced when compared to CRSII, as showed in Fig. 1A (sCrea hAFS $p = 0.07$, rSVC-GFP $p = 0.024$ and NGAL hAFS $p = 0.07$, rSVC-GFP $p = 0.05$ vs CRSII respectively).

3.2. Assessment of kidney damage (histology - apoptosis)

CRSII rats showed histological signs of tubular necrosis and dilatation with nuclear loss without presence of fibrosis, as seen in Fig. 1B. In cell-treated rats tubular size seem to be similar to that of controls with no sign of dilatation (Fig. 1B;b,e and h). CRSII rats showed tubular dilatation, an early histological marker of tubular damage, as highlighted by Fig. 1B,f. In cell-treated rats we found a positive remodeling of tubuli, which seems to maintain the epithelium integrity similar to those of controls (Fig. 1B; c,i). In all groups, no glomerular damage was evident.

Apoptosis data are reported in Fig. 1 and Table 1 in Data in Brief article. The number of apoptotic nuclei in CRSII was 11 folds greater than in controls group (CRSII 82.58 ± 25.01 TUNEL + cells/mm^2 vs controls 7.601 ± 7.11 TUNEL + cells/mm^2, $p = 0.036$ Table 1 in data in brief article). A significant decrease of apoptotic cells was seen in the cell-treated animals (hAFS 14.07 ± 1.38 and rSVC-GFP 12.67 ± 2.69 TUNEL + cells/mm^2 Table 1 in data in brief article).

The differential count of apoptotic nuclei in the kidney cortex and medulla, showed that damage was prevalent in the medulla, where tubules are mainly located. In fact in accordance with the histological features, no difference in apoptosis in the cortex of the cell-treated animals compared to CRSII group was detected. Apoptotic nuclei in the medulla of hAFS and rSVC-GFP groups showed a significant decrease compared to CRSII group (26.4 ± 3.01 and 25.46 ± 6.35 TUNEL + cells/mm^2, $p = 0.03$ vs CRSII 82.58 ± 25.01 TUNEL + cells/mm^2, Table 1 in data in brief article).

A significant ($p < 0.0008$) correlation was found between the number of apoptosis in the medulla and sNGAL confirming the hypothesis that tubular damage due to congestion plays a pivotal pathophysiological role in CRSII.

3.3. Inflammatory citokines

Fig. 2 (in data in brief article) shows the serum levels of pro and anti-inflammatory cytokines. The TNF-α, IL-1α, IL-6 and IL-10 levels were significantly increased in CRSII animal when compared to controls. Cell-treatment brought about significant changes of TNF-α ($p = 0.049$), IL-6 ($p = 0.032$) and IL-10 ($p = 0.031$) levels with the exception of IL-1α that came out to show only a trend to difference ($p = 0.079$). However, changes in cytokine levels were more marked in the rSVC-GFP animals.

3.4. Tissue NGAL in kidneys and heart

Western blot of heart and kidney samples performed both in reducing and denaturing conditions revealed the presence of 25 and the 50 kDa bands, which correspond to monomers and dimers of NGAL (Fig. 2a and f). The optical density of heart and kidney NGAL was 2.3 and 2.4 fold-higher in CRSII ($4.51 \times 10^7 \pm 0.67$ A.U. in heart and $5.13 \times 10^6 \pm 1.51 \times 10^6$ A.U. in kidney) than in controls ($1.93 \times 10^7 \pm 0.64 \times 10^7$ A.U. in heart, $2 \times 10^6 \pm 1.4 \times 10^6$ A.U. in kidney, $p = 0.0079$ and $p = 0.00014$ respectively) (Fig. 2e and l). In CRSII tissues, western blot for MMP9 protein of the same samples revealed the presence of bands at 115, 130 ad 210–220 kDa, representing the complexed forms of NGAL/MMP9 (Fig. 2 b and g). Western blot of kidney and heart samples, performed both in non-reducing and in non-denaturing conditions, confirmed the presence of the NGAL/MMP9 complexes in CRSII group (Fig. 2c,d and h,i) thus enhancing MMP9 protease tissue activity.

In the kidney, semi quantitative optical density in cell-treated rats showed a significantly decrease in NGAL ($2.06 \times 10^6 \pm 1.2 \times 10^6$ A.U. $p = 0.0036$ hAFS and $1.89 \times 10^6 \pm 0.77 \times 10^6$ A.U. $p < 0.0001$in rSVC-GFP vs CRSII, Fig. 2e). Similarly in the heart of cell-treated rats, semi quantitative optical density showed a significant decrease of NGAL levels $2.56 \times 10^6 \pm 1.18 \times 10^6$ A.U., $p = 0.0017$ hAFS and

A

	LVM/RVM	RVM/RVVol	BNP (ng/mL)	sNGAL (ng/mL)	sCreatinina (pg/mL)
Controls	2.838 ± 0.354[a]	2.536 ± 0.771[a]	1.427 ± 0.422[a]	245.3±154[f]	0.5±0.6[i]
CRSII	1.584 ± 0.156[a,b]	1.347 ± 0.241[a,c,d]	4.833 ± 1.329[a,b,e]	532.7±280[f,g,h]	3.5±3.3[i,l,m]
hAFS	2.084 ± 0.200[b]	2.184 ± 1.01[c]	2.314 ± 0.793[b]	357.9±82.7[g]	0.3±0.2[l]
rSVC-GFP	2.164 ± 0.274[a]	2.249 ± 0.723[d]	2.345 ± 1.025[e]	335.6±92.60[h]	0.36±0.05[m]

B

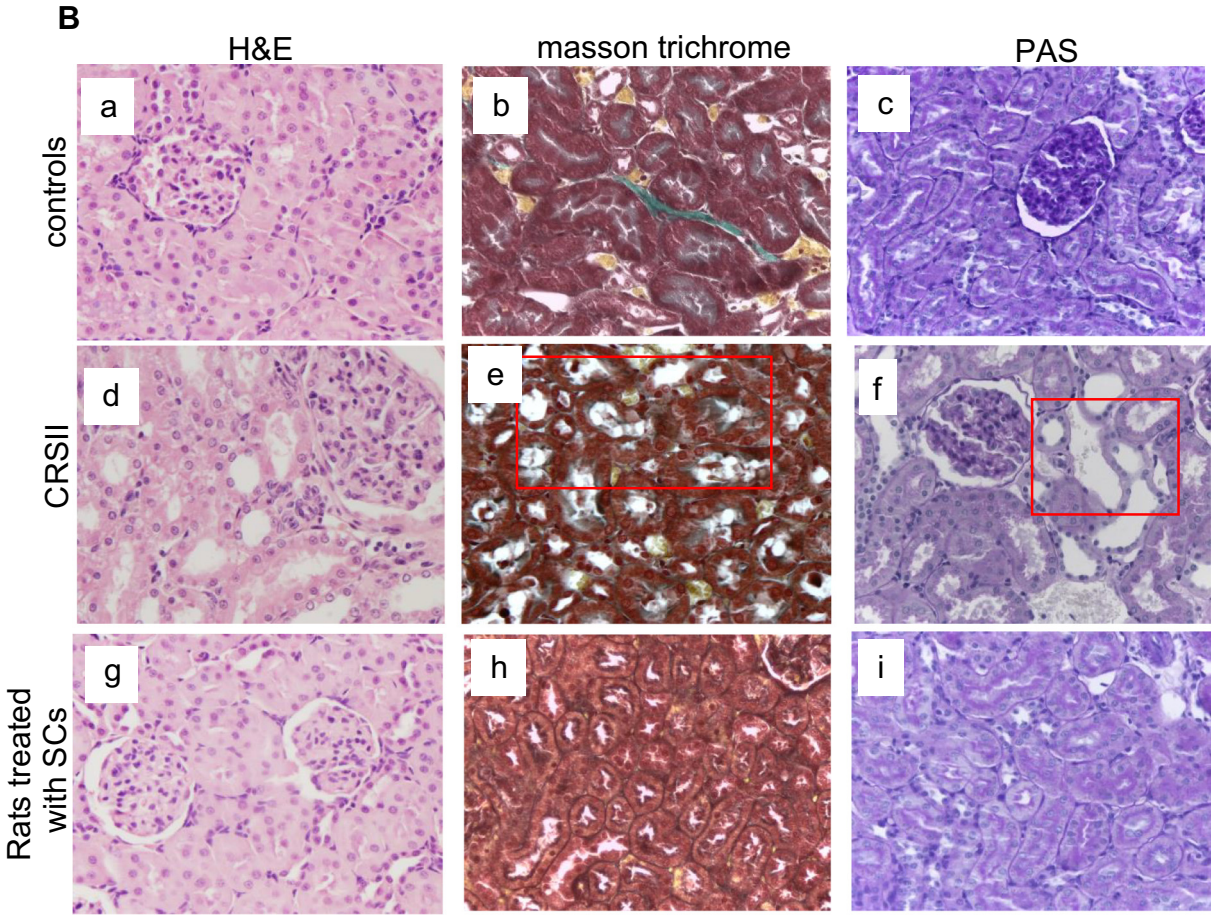

Fig. 1. Heart and Kidney remodeling. A) Occurrence of heart failure and cardiac remodeling: CRSII, cardiorenal syndrome type II rats. hAFS and rSVC-GFP, rats treated with stem cells. a, $p < 0.0001$ (CRSII vs controls and CRSII vs rSVC-GFP respectively); b, $p = 0.0012$ (CRSII vs hAFS);c, $p = 0.0379$ (CRSII vs hAFS);d, $p = 0.0041$ (CRSII vs rSVC-GFP);e, $p = 0.0038$ (CRSII vs rSVC-GFP);f, $p = 0.02$ (CRSII vs controls);g, $p = 0.07$ (CRSII vs hAFS);h, $p = 0.05$ (CRSII vs rSVC-GFP);i, $p = 0.012$ (CRSII vs controls);l, $p = 0.07$ (CRSII vs hAFS); m, $p = 0.024$ (CRSII vs rSVC-GFP); B) Histological kidney remodeling. a, d, and g. H&E staining showing the absence of glomerular damage, interstitial and vascular lesions in all experimental groups of rats. Original magnification 32×; b,e and h Masson trichrome staining showing tubular dilatation in CRSII rats compared to controls without presence of fibrosis. Note as in cell-treated rats tubular seem to be similar to that to controls with no significantly signs of dilatation. Original magnification 32×; c,f and I Periodic acid-Shiff (PAS) staining highlighting tubular epithelial dilatation, an early histological marker of tubular damage, in CRSII rats. In cell-treated rats we found a positively remodeling of tubuli, which seem to maintain the epithelium integrity. Original magnification 32×.

$2.25 \times 10^6 \pm 1.03 \times 10^6$ A.U., $p = 0.0051$ rSVC-GFP vs CRSII rats, Fig. 2l. In cell-treated rats, Western blot for NGAL and MMP9 proteins of kidney and heart samples performed in non-reducing and non-denaturing conditions, showed only faint bands at 115, 130 and 220 kDa, demonstrating a reduction in NGAL/MMP9 complexes (Fig. 2c,d and h,i) thus favoring the inhibition of MMP9 degradation activity and the negative remodeling.

3.5. Transplanted cells engraftment and differentiation

The transplanted cells that passed the pulmonary filter (Fig. S1) engrafted in different organs as follows: Lung: hAFS: 13 ± 2; rSVC-GFP: 56 ± 5 mm^2 (Fig. S1); Heart: hAFS: 3,5 ± 0,3; rSVC-GFP: 1,2 ± 0,8 mm^2; Skeletal muscle hAFS: 2,3 ± 0,4; rSVC-GFP: 8,9 ± 0,7 mm^2.

The number of engrafted cells, in the Kidney, is reported in Fig. 3l and m. The total number of engrafted rSVC-GFP cells (5.45 ± 1.1 cells/mm^2) was similar to that of hAFS (4.052 ± 0.96 cells/mm^2). We observed that the engrafted cells differentiated or fused into endothelial, SMA cells and kidney tubuli (Fig. 3 a through i). A considerable number of stem cells were found in the interstitium. In general hAFS showed a higher number of interstitial positive cells than rSVC-GFP ($p = 0.043$) which seems to be more prone to differentiate in tubular-cells ($p = 0.002$) as showed in histogram reported in Fig. 3l. Both type of stem cells are able to differentiate in endothelial and SMA positive cells with a higher number of differentiated cells originating from rSVC-GFP, compared to hAFS, even though

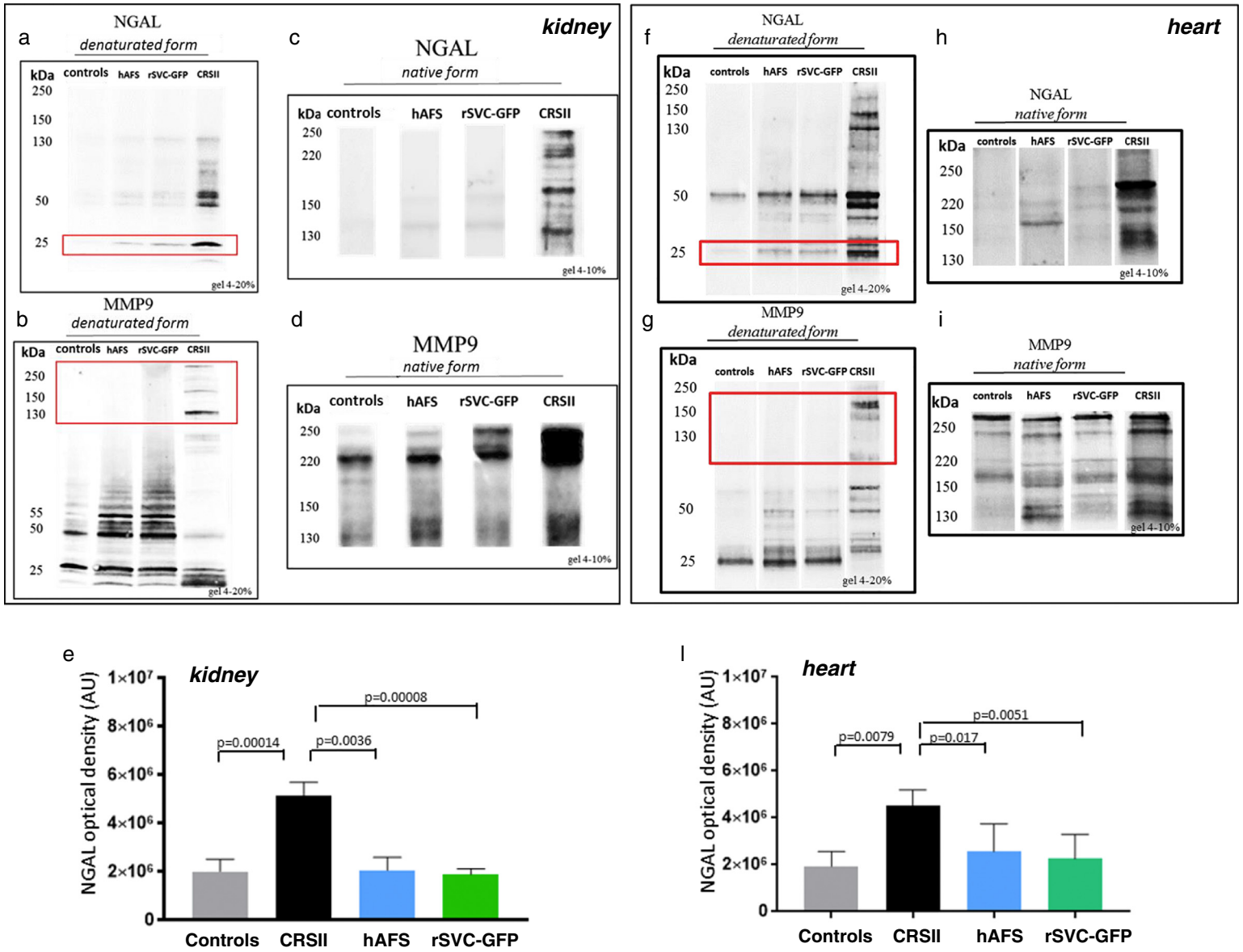

Fig. 2. Tissue NGAL in kidney. a,f) Representative Western blots for NGAL detection in kidneys and heart performed in reducing and denaturing conditions. Western blot revealed the presence of 25 and 50 kDa bands, which correspond to monomers and dimers of NGAL protein. Note also the presence, in the CRSII rats, of 130 kDa-band, which represent the complexed NGAL/MMP9; b,g) representative Western blots, of the same sample, for MMP9 detection in kidney and heart performed in reducing and denaturing conditions. Western blot revealed the presence of 50–55 kDa band, which correspond to MMP9 monomer. In CRSII rats we found also bands at 115 kDa, 130 and 220 kDa (red inset), representing the complexed forms of NGAL/MMP9. Cell-treated rats do not show bands which correspond to NGAL/MMP9 complexes; c, d, h and i) representative western blots in non –reducing and in non-denaturating conditions (that preserved the native complexes form), confirming the presence of the complexes NGAL/MMP9 in CRSII rats groups compared to controls. Conversely, cell-treated rats show only faint bands on 130 kDa suggesting a positive remodeling on kidney. e) semi quantitative optical density of NGAL in kidney, expressed by arbitrary unit (A.U.), which support the data of western blot images. Cell-treated rats show a significantly decrease in the NGAL release ($p = 0.0036$ hAFS and $p < 0.0001$ rSVC-GFP vs CRSII rats); l) semi quantitative optical density of NGAL in heart, expressed by arbitrary unit (A.U.), which support the data of western blot images. Cell-treated rats show a significant decrease in the NGAL release ($p = 0.0017$ hAFS and $p = 0.0051$ rSVC-GFP vs CRSII rats).

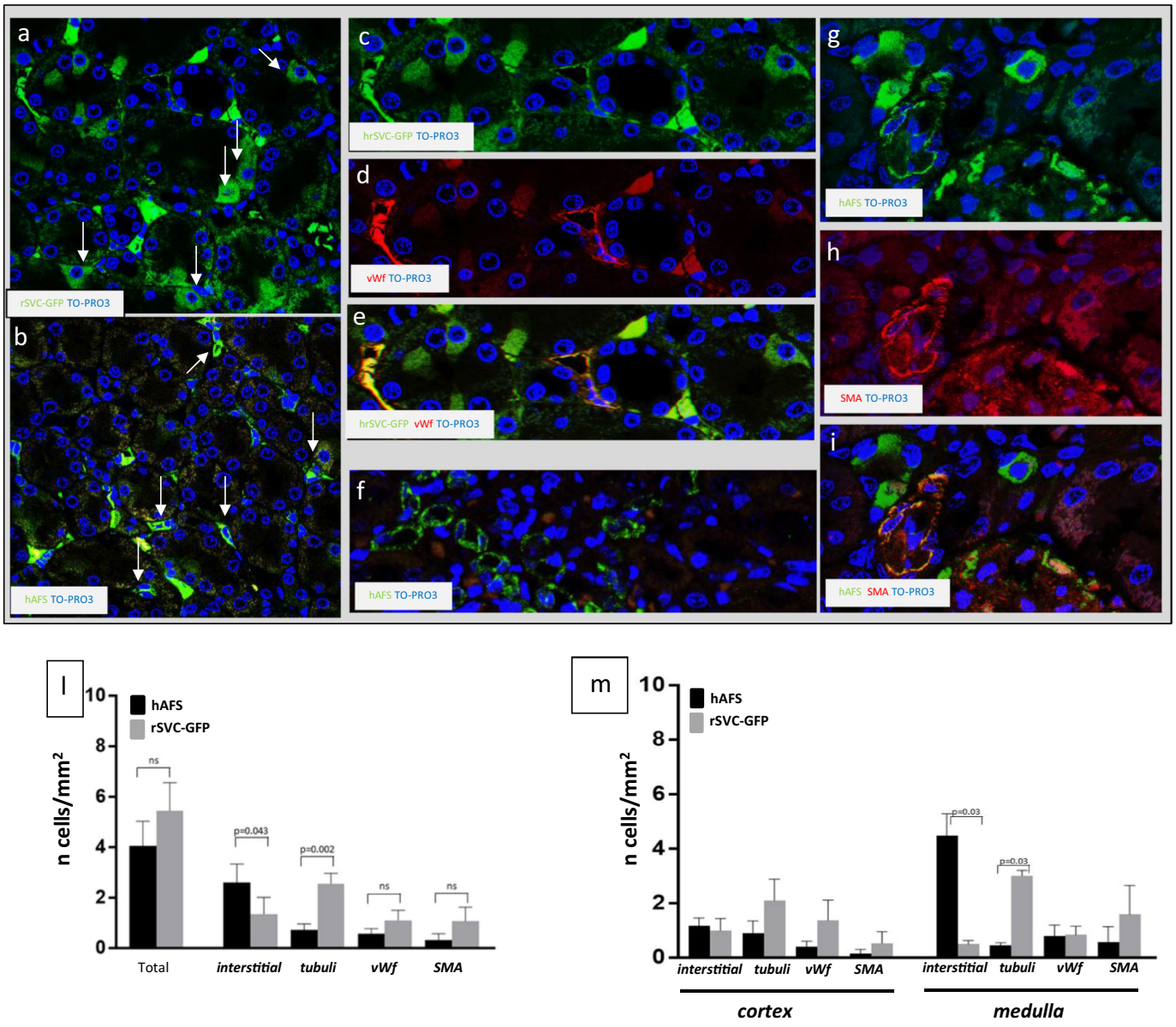

Fig. 3. Stem Cells Engraftment: Representative Confocal images showing the stem cells engraftment in kidney. a) confocal image depicting rSVC-GFP differentiated and integrated in tubuli (white arrows) (rSVC-GFP in green and cells nuclei in blue). Original magnification 40×;b) confocal image showing hAFS engrafted as scattered cells in interstitium (hAFS in green and cell nuclei in blue). Original magnification 40×. note as rSVC-GFP stromal stem cells are more prone to differentiate into tubular cells than hAFS which remain in the interstitium as showed also by cells quantification reported in l and m; c,d,e and f) an example of confocal images depicting the cell differentiation into endothelial cells (c,d and e rSVC-GFP stem cells, and hAFS in f). The α vWf in red was followed by counterstaining with TO-PRO3 (nuclei in blue). α vWf cells were identified by the merge section with co-localization in yellow. Zoom from original magnification of 40×; g,h and i) confocal image showing hAFS differentiation in a new tubul and in an arteriola. SMA in red was followed by counterstaining with TO-PRO3 (nuclei in blue). Smooth muscle cells were identified by the merge section with co-localization in yellow. Zoom from original magnification; l and m) histograms show stem cells engraftment quantification. In l is reported a total quantification divided for hAFS and rSVC-GFP. Note as rSVC-GFP stem cells are able to differentiate in kidney tubular cells compared to hAFS ($p = 0.002$). Histogram in m shows the stem cells engraftment separate by cortex and medulla region of kidney. Note as the main stem cells differentiation in tubuli takes place in the medulla region. Both type of stem cells are able to differentiate in vWf and SMA cells, making angiogenesis and vasculogenesis.

statistical significance difference was not reached. Fig. 3m shows the distribution of stem cells engraftment in the cortical and medulla region of the kidney. The two groups of cell-treatment showed the same degree of differentiation into renal tubuli and endothelial cells in the cortex. On the contrary, in the medulla there was a difference in terms of cell differentiation. In fact rSVC-GFP group showed higher number of tubuli positive cells (3.0 ± 0.19 cells/mm^2) compared to hAFS (0.45 ± 0.09 cells/mm^2, $p = 0.03$ Fig. 3m). There was a higher number of undifferentiated hAFS at interstitial level (4.47 ± 0.8 cells/mm^2) when compared to rSVC-GFP group (0.5 ± 0.14 cells/mm^2, $p = 0.03$). No statistically significant differences were seen for vWf and SMA differentiation for both hAFS (vWf 0.79 ± 0.39 cells/mm^2, SMA 0.57 ± 0.56 cells/mm^2) and rSVC-GFP groups (vWf 0.84 ± 0.32 cells/mm^2, SMA 1.5 ± 1.05 cells/mm^2, $p =$ ns) even though there was a trend for higher differentiation potential for rSVC-GFP group (Fig. 3m).

4. Discussion

In this well characterized model of RV failure secondary to pulmonary hypertension [18,26] and systemic congestion, kidney injury occurred as demonstrated by the increased levels of sCreatinine and sNGAL. Clinical signs of congestion such as pleural effusion and ascites were present. Right heart failure developed as demonstrated by the RV dilatation, eccentric hypertrophy and elevated levels of BNP,

suggesting that the criteria for CRS type II, i.e. the presence of kidney damage secondary to heart failure, were met.

A systemic inflammatory response was detected as the circulating level of pro-inflammatory cytokines was increased.

The functional impairment of kidney was accompanied by a structural damage that consisted of tubular damage and increased of apoptosis.

Apoptosis was mostly confined in the medulla and particularly in tubular cells and is likely to be activated by the high levels of circulating cytokines.

Tubular disruption and dilatation was seen at histology. It is reasonable that a secondary release of NGAL protein occurred. This is very likely due to the increased pressure in the medulla, due to congestion.

In our animals no histologic evidence of glomerular damage or inflammatory cells infiltrate was detected. This supports the hypothesis that kidney damage is mediated by circulating and tissue cytokines rather than local cellular-mediated inflammation.

We can discuss on the origin of inflammation in cardiac failure, and several hypotheses have been put forward. The heart itself can produce tumor necrosis factor, sphingosine and other cytokines [26,34,35].

Other authors suggest that the neuroendocrine activation, characterized by increased levels of catecholamine and angiotensin II may induce cytokine release.

Congestion itself can induce cytokine release by the gut [36,37] through production of LPS.

The role of oxidative stress has been advocated as well [38,39].

Our group has already shown in patients with CRS type I the role of circulating monocytes in producing cytokines and apoptosis. Moreover sera of patients with CRS type I produced apoptosis in cultured tubular cells [40,41].

Kidney congestion may lead to production of cytokines, especially IL6, that may be in turn responsible for apoptosis itself [42,43]. Moreover Du et al. [44] have shown that tubular cells themselves can under hypoxic stimuli produce proinflammatory and profibrotic factors.

NGAL, which is produced by kidney tubuli after injury, is a biomarker used to monitor renal tubular damage even in the absence of significant reduction of GFR parameters [45–47]. NGAL cannot be considered a sole biomarker, but is an important effector in the kidney-heart cross talk as demonstrated in our previous work [3] in that it is able to produce further negative heart remodeling by activating metalloproteinases. NGAL (a specific MMP9 binder) binds MMP9 in both heart and kidney, avoiding the metalloproteinase degradation with enhancement of its enzymatic activity, leading to increased collagen breakdown with consequent negative heart remodeling [3]. In the present paper we demonstrated that cell-therapy prevents the formation of NGAL/MMP9 complexes suggesting a positive remodeling on kidney and heart. Cell-treatment showed a significantly decrease in kidney NGAL release and a consequent reduction in NGAL/MMP9 complex formation.

These findings confirm that NGAL cannot be seen as a simple biomarker of kidney damage, but, in turn, as an actor in determining heart and kidney cross-talk and remodeling.

Combined with a reduction in renal NGAL, cell-treatment also leads to a decrease in apoptosis, mainly in the medulla. Cell-therapy produced striking effects on kidney function. In fact serum creatinine and NGAL decreased significantly in both hAFS and rSVC-GFP group.

The observed reduction of circulating cytokines may be responsible for the beneficial effect detected in the kidney and in the heart. This is an important aspect of the heart-kidney cross-talk. However, we cannot exclude that local release or production of cytokines may have had a paracrine effect with positive consequences on apoptosis, cell engraftment and differentiation. Indeed the paracrine effect of hAFS has been documented both in cardiac and kidney regeneration [48,49] . Also in this model, we can foresee a paracrine effect of both injected cells since their percentage found post injection is not extremely high as well as the cells positive for human mitochondria antigen.

Importantly, an improvement in histologic signs of tissue damage was detected. Apoptosis was reduced in tubular, vascular and interstitial cells, suggesting that changes in the pro-inflammatory milieu could have produced prevention of apoptosis. This explains part of the improvement in kidney damage simply by blocking the apoptotic cell death.

On the other side, we observed stem cells engraftment and differentiation.

Tubular cells regeneration, together with SMC and endothelial cell repopulation was present as demonstrated by the specific double staining for vWF and SMA, anti GFP antibodies and anti-human mitochondrial antibodies.

In this paper we used the stem cells from amniotic fluid and the vascular stromal fraction cells. Previous authors have compared hAFS stem cells with bone-marrow mesenchymal stem cells [50] showing that hAFS had more potent anti-apoptotic activity against renal tubular cells but lesser stimulatory activity for the proliferation/differentiation into renal tubular cells. In our paper, by comparing hAFS and rSVC-GFP, we did not find differences on the inflammatory milieu, in terms of cytokines profile and anti-apoptotic activity. hAFS showed more engraftment as SC in the interstitium and less tubular differentiation. A trend toward less endothelial and vascular differentiation was evident. This is probably due to the fact that hAFS represent a more heterogeneous population of non-committed stem cells when compared to many adult progenitor cell types such as bone marrow or adipose derived stem cells or as our vascular stromal cells.

We cannot exclude stem cells fusion as a mechanism of engraftment and differentiation as suggested by Du [44]. This may represent a major reno-protective effect.

We can ascribe the different degree of apoptosis and cell differentiations in the medulla compared to the cortex to the higher medullar tubular damage, which is the result of the pathophysiology of CRSII in this animal model.

5. Conclusions

In the present study, we have demonstrated that cell therapy with both human amniotic stem cells and vascular stromal cells is able to improve kidney function and restore kidney structure. We have also produced evidences that cell-therapy, by reducing NGAL and its effect on MMP9 at cardiac and kidney levels, could prevent negative remodeling by acting on metalloproteinases thus reinforcing the importance of breaking the vicious cross talk circle between kidney and heart, which represents a pathophysiological mechanism of function deterioration in CRSII.

Cell-therapy treatment act through two different mechanisms:

1) a paracrine mechanism with anti-inflammatory and anti-apoptotic effect
2) engraftment and differentiation of stem cells with repopulation of tubular, endothelial, SMA and interstitial cells (see Fig. 4 pathophysiology of cardio-renal syndrome and cells repair)

We think that the mechanisms involved in the amelioration of kidney function are complex, comprising the direct effect of engrafted cells in the damaged organ, the paracrine effect of the injected stem cell, the improvement of cardiac and vascular function. The contribution of each factor is at the moment impossible to be weighed.

Future research on stem cells therapy should focus on a better understanding of their mechanisms of action. In other words whether cells really need to reach the diseased organ and engraft or if an hit-and-run effect through a paracrine action (microparticles, miRNA, exosomes) that may block apoptosis or mitigate tissue damage and

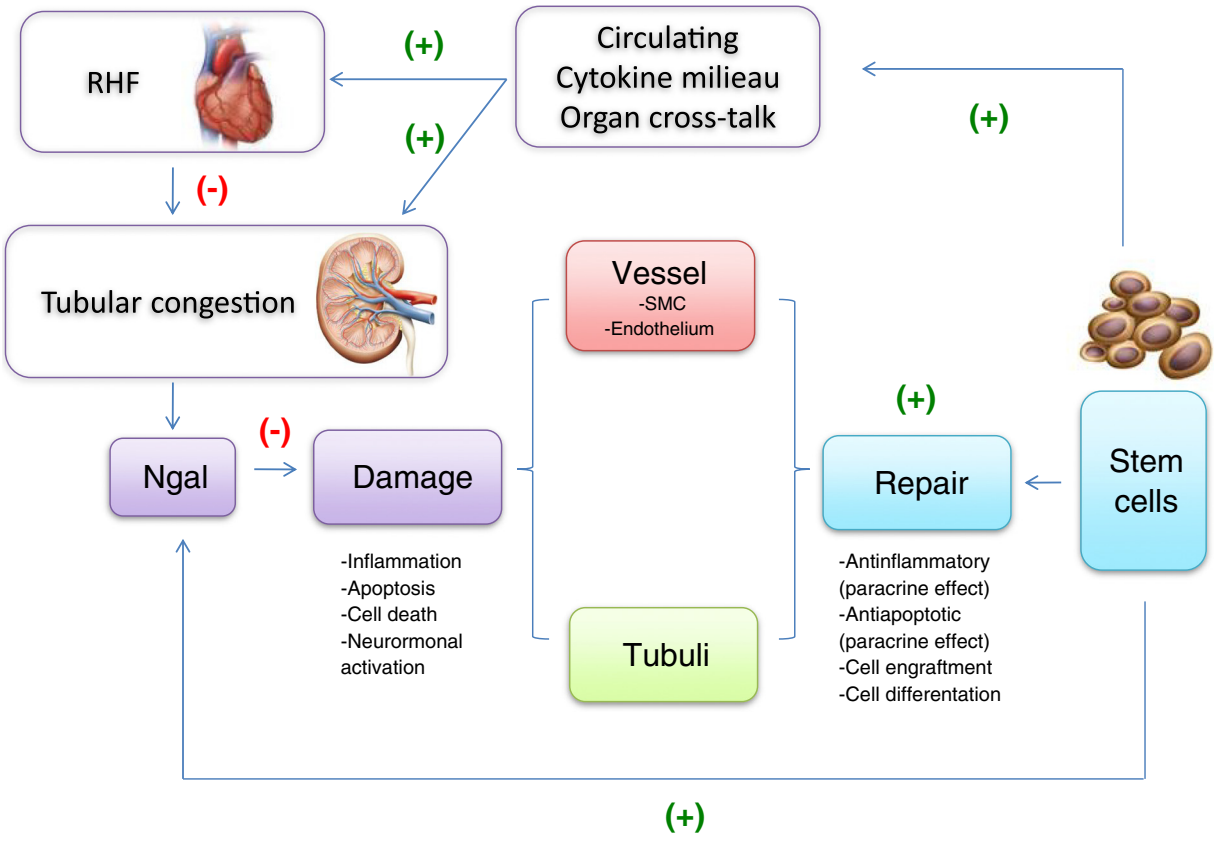

Fig. 4. Stem cells mechanisms of injury and repair in CRSII Cell-therapy is able to: 1) Produce anti-inflammatory and anti-apoptotic renal effects (paracrine) 2) Produce cell engraftment and differentiation with regeneration of vascular and tubular cells 3) Reduce circulating cytokines with effects on organ cross-talk 4) Reduce kidney, circulating and heart NGAL with secondary effects on MMP9 and prevention of negative cardiac remodeling.

inflammation by modulating the immune system and resident stem cells is necessary to exert a beneficial effect.

Supplementary data to this article can be found online at https://doi.org/10.1016/j.ijcard.2018.10.038.

Acknowledgement and sources of funding

The authors thank Elisabetta Baliello and Alessandra Dubrovich for their skillful technical assistance.

Conception and design of the research: GV, AA, CC; acquisition of data: CC, GM Vescovo, MP, RT, MF, GM Virzì; analysis and interpretation of the data: GV, CC, AA; statistical analysis, GMV, GG, CC; obtaining funding and supervising the work: GV, AA; drafting the manuscript: GV, CC and AA; critical revision of the manuscript for important intellectual content: GV and AA.

This work was supported by research grants from the Veneto Region (RF-VEN303/09) and from the University of Padua (60A07-0104/14 and 60A07-0945/15 as well as GRIC13IH1H). The authors of this manuscript have certified that they comply with the Principles of Ethical Publishing in the International Journal of Cardiology.

The authors declare that they have not conflicts of interest.

References

[1] C. Ronco, P. McCullough, S.D. Anker, I. Anand, N. Aspromonte, S.M. Bagshaw, R. Bellomo, T. Berl, I. Bobek, D.N. Cruz, L. Daliento, A. Davenport, M. Haapio, H. Hillege, A.A. House, N. Katz, A. Maisel, S. Mankad, P. Zanco, A. Mebazaa, A. Palazzuoli, F. Ronco, A. Shaw, G. Sheinfeld, S. Soni, G. Vescovo, N. Zamperetti, P. Ponikowski, Acute Dialysis Quality Initiative (ADQI) Consensus Group, Cardio-renal syndromes: report from the consensus conference of the acute dialysis quality initiative, Eur. Heart J. 31 (2010) 703–711, https://doi.org/10.1093/eurheartj/ehp507.

[2] C. Ronco, M. Haapio, A.A. House, N. Anavekar, R. Bellomo, Cardiorenal syndrome, J. Am. Coll. Cardiol. 52 (2008) 1527–1539, https://doi.org/10.1016/j.jacc.2008.07.051.

[3] A. Angelini, C. Castellani, G.M. Virzì, M. Fedrigo, G. Thiene, M. Valente, C. Ronco, G. Vescovo, The role of congestion in cardiorenal syndrome type 2: new pathophysiological insights into an experimental model of heart failure, Cardiorenal Med. 6 (2015) 61–72, https://doi.org/10.1159/000440775.

[4] J. Preeti, M. Alexandre, I. Pupalan, T.C. Merlin, C. Ronco, Chronic heart failure and comorbid renal dysfunction - a focus on type 2 cardiorenal syndrome, Curr. Cardiol. Rev. 12 (2016) 186–194, https://doi.org/10.2174/1573403X12666160606120958.

[5] D.N. Cruz, K.M. Schmidt-Ott, G. Vescovo, A.A. House, J.A. Kellum, C. Ronco, P.A. McCullough, Pathophysiology of cardiorenal syndrome type 2 in stable chronic heart failure: workgroup statements from the eleventh consensus conference of the acute dialysis quality initiative (ADQI), Contrib. Nephrol. 182 (2013) 117–136, https://doi.org/10.1159/000349968.

[6] C. Castellani, G. Vescovo, B. Ravara, C. Franzin, M. Pozzobon, R. Tavano, L. Gorza, E. Papini, R. Vettor, P. De Coppi, G. Thiene, A. Angelini, The contribution of stem cell therapy to skeletal muscle remodeling in heart failure, Int. J. Cardiol. 168 (2013) 2014–2021, https://doi.org/10.1016/j.ijcard.2013.01.168.

[7] A. Angelini, C. Castellani, B. Ravara, C. Franzin, M. Pozzobon, R. Tavano, L.D. Libera, E. Papini, R. Vettor, P. De Coppi, G. Thiene, G. Vescovo, Stem-cell therapy in an experimental model of pulmonary hypertension and right heart failure: role of paracrine and neurohormonal milieu in the remodeling process, J. Heart Lung Transplant. 30 (2011) 1281–1293, https://doi.org/10.1016/j.healun.2011.07.017.

[8] A. Zarjou, J. Kim, A.M. Traylor, P.W. Sanders, J. Balla, A. Agarwal, L.M. Curtis, Paracrine effects of mesenchymal stem cells in cisplatin-induced renal injury require heme oxygenase-1, Am. J. Physiol. Renal Physiol. 300 (1) (2011) F254–F262, https://doi.org/10.1152/ajprenal.00594.2010.

[9] J. Feng, C. Lu, Q. Dai, J. Sheng, M. Xu, SIRT3 facilitates amniotic fluid stem cells to repair diabetic nephropathy through protecting mitochondrial homeostasis by modulation of mitophagy, Cell. Physiol. Biochem. 46 (4) (2018) 1508–1524, https://doi.org/10.1159/000489194.

[10] H. Yang, X. Zhang, G. Xin, Investigation of mechanisms of mesenchymal stem cells for treatment of diabetic nephropathy via construction of a miRNA-TF-mRNA network, Ren. Fail. 40 (1) (2018) 136–145, https://doi.org/10.1080/0886022X.2017.1421556.

[11] Y. Li, J. Liu, G. Liao, J. Zhang, Y. Chen, L. Li, L. Li, F. Liu, B. Chen, G. Guo, C. Wang, L. Yang, J. Cheng, Y. Lu, Early intervention with mesenchymal stem cells prevents nephropathy in diabetic rats by ameliorating the inflammatory microenvironment, Int. J. Mol. Med. 41 (5) (2018) 2629–2639, https://doi.org/10.3892/ijmm.2018.3501.

[12] H.H. Anan, R.A. Zidan, M.A. Shaheen, E.A. Abd-El Fattah, Therapeutic efficacy of bone marrow derived mesenchymal stromal cells versus losartan on adriamycin-induced

renal cortical injury in adult albino rats, Cytotherapy 18 (2016) 970–984, https://doi.org/10.1016/j.jcyt.2016.05.004.
[13] L. Li, P. Truong, P. Igarashi, F. Lin, Renal and bone marrow cells fuse after renal ischemic injury, J. Am. Soc. Nephrol. 18 (12) (2007) 3067–3077, https://doi.org/10.1681/ASN.2007030284.
[14] T. Yamashita, M. Fujimiya, K. Nagaishi, K. Ataka, M. Tanaka, H. Yoshida, K. Tsuchihashi, K. Shimamoto, T. Miura, Fusion of bone marrow derived cells with renal tubules contributes to renal dysfunction in diabetic nephropathy, FASEB J. 26 (4) (2012) 1559–1568, https://doi.org/10.1096/fj.11-183194.15.
[15] A.Q. Lam, B.S. Freedman, R. Morizane, P.H. Lerou, M.T. Valerius, J.V. Bonventre, Rapid and efficient differentiation of human pluripotent stem cells into intermediate mesoderm that forms tubules expressing kidney proximal tubular markers, J. Am. Soc. Nephrol. 25 (6) (2014) 1211–1225, https://doi.org/10.1681/ASN.201308083116.
[16] L.A. Reis, F.T. Borges, M.J. Simoes, A.A. Borges, R. Sinigaglia-Coimbra, N. Schor, Bone marrow-derived mesenchymal stem cells repaired but did not prevent gentamicin-induced acute kidney injury through paracrine effects in rats, PLoS One 7 (9) (2012), e44092. https://doi.org/10.1371/journal.pone.0044092.
[17] J.J. Rivera Valdes, J. García-Bañuelos, A. Salazar-Montes, L. García-Benavides, A. Rosales-Dominguez, J. Armendáriz-Borunda, A. Sandoval-Rodríguez, Human adipose derived stem cells regress fibrosis in a chronic renal fibrotic model induced by adenine, PLoS One 12 (12) (2017), e0187907. https://doi.org/10.1371/journal.pone.0187907.
[18] L. Dalla Libera, B. Ravara, A. Angelini, K. Rossini, M. Sandri, G. Thiene, G. Battista Ambrosio, G. Vescovo, Beneficial effects on skeletal muscle of the angiotensin II type 1 receptor blocker irbesartan in experimental heart failure, Circulation 103 (2001) 2195–2200, https://doi.org/10.1161/01.CIR.103.17.2195.
[19] G. Vescovo, B. Ravara, V. Gobbo, L. Dalla Libera, Inflammation and perturbation of the L-carnitine system in heart failure, Eur. J. Heart Fail. 7 (6) (2005) 997–1002, https://doi.org/10.1016/j.ejheart.2004.11.010.
[20] G. Vescovo, B. Ravara, V. Gobbo, A. Angelini, L. Dalla Libera, Skeletal muscle fibres synthesis in heart failure: role of PGC-1alpha, calcineurin and GH, Int. J. Cardiol. 104 (3) (2005) 298–306, https://doi.org/10.1016/j.ijcard.2004.10.059.
[21] L. Dalla Libera, B. Ravara, V. Gobbo, D. Danieli Betto, E. Germinario, A. Angelini, G. Vescovo, Skeletal muscle myofibrillar protein oxidation in heart failure and the protective effect of carvedilol, J. Mol. Cell. Cardiol. 38 (5) (2005) 803–807, https://doi.org/10.1016/j.yjmcc.2005.02.023.
[22] L. Dalla Libera, B. Ravara, M. Volterrani, V. Gobbo, M. Della Barbera, A. Angelini, D. Danieli Betto, E. Germinario, G. Vescovo, Beneficial effects of GH/IGF-1 on skeletal muscle atrophy and function in experimental heart failure, Am. J. Physiol. Cell Physiol. 286 (1) (2004) C138–C144, https://doi.org/10.1152/ajpcell.00114.2003.
[23] G. Vescovo, B. Ravara, V. Gobbo, M. Sandri, A. Angelini, M. Della Barbera, M. Dona, G. Peluso, M. Calvani, L. Mosconi, L. Dalla Libera, L-Carnitine: a potential treatment for blocking apoptosis and preventing skeletal muscle myopathy in heart failure, Am. J. Physiol. Cell Physiol. 283 (3) (2002) C802–C810, https://doi.org/10.1152/ajpcell.00046.2002.
[24] G. Vescovo, B. Ravara, A. Angelini, M. Sandri, U. Carraro, C. Ceconi, L. Dalla Libera, Effect of thalidomide on the skeletal muscle in experimental heart failure, Eur. J. Heart Fail. 4 (4) (2002) 455–460, https://doi.org/10.1016/S1388-9842(02)00022-3.
[25] L. Dalla Libera, R. Sabbadini, C. Renken, B. Ravara, M. Sandri, R. Betto, A. Angelini, G. Vescovo, Apoptosis in the skeletal muscle of rats with heart failure is associated with increased serum levels of TNF-alpha and sphingosine, J. Mol. Cell. Cardiol. 33 (10) (2001) 1871–1878, https://doi.org/10.1006/jmcc.2001.1453.
[26] G. Vescovo, R. Zennaro, M. Sandri, U. Carraro, C. Leprotti, C. Ceconi, G.B. Ambrosio, L. Dalla Libera, Apoptosis of skeletal muscle myofibers and interstitial cells in experimental heart failure, J. Mol. Cell. Cardiol. 30 (11) (1998) 2449–2459, https://doi.org/10.1006/jmcc.1998.0807.
[27] P. De Coppi, G. Bartsch Jr., M.M. Siddiqui, T. Xu, C.C. Santos, L. Perin, G. Mostoslavsky, A.C. Serre, E.Y. Snyder, J.J. Yoo, M.E. Furth, S. Soker, A. Atala, Isolation of amniotic stem cell lines with potential for therapy, Nat. Biotechnol. 25 (2007) 100–106, https://doi.org/10.1038/nbt1274.
[28] C. Rota, B. Imberti, M. Pozzobon, M. Piccoli, P. De Coppi, A. Atala, E. Gagliardini, C. Xinaris, V. Benedetti, A.S. Fabricio, E. Squarcina, M. Abbate, A. Benigni, G. Remuzzi, M. Morigi, Human amniotic fluid stem cell preconditioning improves their regenerative potential, Stem Cells Dev. 21 (2012) 1911–1923, https://doi.org/10.1089/scd.2011.0333.
[29] R. Madonna, L.W. Van Laake, S.M. Davidson, F.B. Engel, D.J. Hausenloy, S. Lecour, J. Leor, C. Perrino, R. Schulz, K. Ytrehus, U. Landmesser, C.L. Mummery, S. Janssens, J. Willerson, T. Eschenhagen, P. Ferdinandy, J.P. Sluijter, Position paper of the European Society of Cardiology Working Group Cellular Biology of the Heart: cell-based therapies for myocardial repair and regeneration in ischemic heart disease and heart failure, Eur. Heart J. 37 (23) (2016) 1789–1798, https://doi.org/10.1093/eurheartj/ehw113.
[30] R. Madonna, Y.J. Geng, R. De Caterina, Adipose tissue-derived stem cells: characterization and potential for cardiovascular repair, Arterioscler. Thromb. Vasc. Biol. 29 (11) (2009) 1723–1729, https://doi.org/10.1161/ATVBAHA.109.187179.
[31] J.M. Gimble, A.J. Katz, B.A. Bunnell, Adipose-derived stem cells for regenerative medicine, Circ. Res. 100 (9) (2007) 1249–1260.
[32] R. Tavano, S. Franzoso, P. Cecchini, E. Cartocci, F. Oriente, B. Aricò, E. Papini, The membrane expression of *Neisseria meningitidis* adhesin A (NadA) increases the proimmune effects of *MenB* OMVs on human macrophages, compared with NadA^{-} OMVs, without further stimulating their proinflammatory activity on circulating monocytes, J. Leukoc. Biol. 86 (2009) 143–153, https://doi.org/10.1189/jlb.0109030.
[33] A. Scarda, C. Franzin, G. Milan, M. Sanna, C. Dal Prà, C. Pagano, L. Boldrin, M. Piccoli, E. Trevellin, M. Granzotto, P. Gamba, G. Federspil, P. De Coppi, R. Vettor, Increased adipogenic conversion of muscle satellite cells in obese Zucker rats, Int. J. Obes. 34 (8) (2010) 1319–1327, https://doi.org/10.1038/ijo.2010.47.
[34] B. Levine, J. Kalman, L. Mayer, H.M. Fillit, M. Packer, Elevated circulating levels of tumor necrosis factor in severe chronic heart failure, N. Engl. J. Med. 323 (1990) 236–241, https://doi.org/10.1056/NEJM199007263230405.
[35] G. Vescovo, L. Dalla Libera, Who has inflamed my heart and makes my body burn? The Othello's dilemma in heart failure, Int. J. Cardiol. 135 (2) (2009) 236–237, https://doi.org/10.1016/j.ijcard.2008.05.016.
[36] L. Cuoco, G. Vescovo, R. Castaman, B. Ravara, G. Cammarota, A. Angelini, M. Salvagnini, L. Dalla Libera, Skeletal muscle wastage in Crohn's disease: a pathway shared with heart failure? Int. J. Cardiol. 127 (2) (2008) 219–227, https://doi.org/10.1016/j.ijcard.2007.06.006.
[37] J. Niebauer, H.D. Volk, M. Kemp, M. Dominguez, R.R. Schumann, M. Rauchhaus, P.A. Poole-Wilson, A.J. Coats, S.D. Anker, Endotoxin and immune activation in chronic heart failure: a prospective cohort study, Lancet 353 (1999) 1838–1842, https://doi.org/10.1016/S0140-6736(98)09286-1.
[38] G.M. Virzi, R. Torregrossa, D.N. Cruz, C.Y. Chionh, M. de Cal, S.S. Soni, M. Dominici, G. Vescovo, M.H. Rosner, C. Ronco, Cardiorenal syndrome type 1 may be immunologically mediated: a pilot evaluation of monocyte apoptosis, Cardiorenal Med. 2 (2012) 33–42, https://doi.org/10.1159/000335499.
[39] G.M. Virzì, A. Clementi, M. de Cal, A. Brocca, S. Day, S. Pastori, C. Bolin, G. Vescovo, C. Ronco, Oxidative stress: dual pathway induction in cardiorenal syndrome type 1 pathogenesis, Oxidative Med. Cell. Longev. 2015 (2015), 391790. https://doi.org/10.1155/2015/391790.
[40] A. Clementi, G.M. Virzì, A. Brocca, M. de Cal, S. Pastori, M. Clementi, A. Granata, G. Vescovo, C. Ronco, Advances in the pathogenesis of cardiorenal syndrome type 3, Oxidative Med. Cell. Longev. 2015 (2015) 148082, https://doi.org/10.1155/2015/148082.
[41] A. Havasi, S.C. Borkan, Apoptosis and acute kidney injury, Kidney Int. 80 (1) (2011) 29–40, https://doi.org/10.1038/ki.2011.120.
[42] P.C. Colombo, A. Ganda, J. Lin, D. Onat, A. Harxhi, J.E. Iyasere, N. Uriel, G. Cotter, Inflammatory activation: cardiac, renal, and cardio-renal interactions in patients with the cardiorenal syndrome, Heart Fail. Rev. 17 (2) (2012) 177–190, https://doi.org/10.1007/s10741-011-9261-3.
[43] R.L. Amdur, M. Mukherjee, A. Go, I.R. Barrows, A. Ramezani, J. Shoji, M.P. Reilly, J. Gnanaraj, R. Deo, S. Roas, M. Keane, S. Master, V. Teal, E.Z. Soliman, P. Yang, H. Feldman, J.W. Kusek, C.M. Tracy, D.S. Raj, Study investigators interleukin-6 is a risk factor for atrial fibrillation in chronic kidney disease: findings from the CRIC study investigators, PLoS One 11 (2) (2016 Feb 3), e0148189. https://doi.org/10.1371/journal.pone.0148189.
[44] T. Du, Y.J. Zhu, The regulation of inflammatory mediators in acute kidney injury via exogenous mesenchymal stem cells, Mediat. Inflamm. 2014 (2014) 261697, https://doi.org/10.1155/2014/261697.
[45] A. Clerico, C. Galli, A. Fortunato, C. Ronco, Neutrophil gelatinase-associated lipocalin (NGAL) as biomarker of acute kidney injury: a review of the laboratory characteristics and clinical evidences, Clin. Chem. Lab. Med. 50 (9) (2012) 1505–1517, https://doi.org/10.1515/cclm-2011-0814.
[46] P.R. Taub, K.C. Borden, A. Fard, A. Maisel, Role of biomarkers in the diagnosis and prognosis of acute kidney injury in patients with cardiorenal syndrome, Expert. Rev. Cardiovasc. Ther. 10 (5) (2012) 657–667, https://doi.org/10.1586/erc.12.26.
[47] M. Nishimura, A. Brann, K.W. Chang, A.S. Maisel, The confounding effects of non-cardiac pathologies on the interpretation of cardiac biomarkers, Curr. Heart Fail. Rep. (2018 Jul 10)https://doi.org/10.1007/s11897-018-0398-4.
[48] C. Rota, B. Imberti, M. Pozzobon, M. Piccoli, P. De Coppi, A. Atala, E. Gagliardini, C. Xinaris, V. Benedetti, A.S. Fabricio, E. Squarcina, M. Abbate, A. Benigni, G. Remuzzi, M. Morigi, Human amniotic fluid stem cell preconditioning improves their regenerative potential, Stem Cells Dev. 21 (11) (2012 Jul 20) 1911–1923, https://doi.org/10.1089/scd.2011.0333.
[49] S. Bollini, K.K. Cheung, J. Riegler, X. Dong, N. Smart, M. Ghionzoli, S.P. Loukogeorgakis, P. Maghsoudlou, K.N. Dubé, P.R. Riley, M.F. Lythgoe, P. De Coppi, Amniotic fluid stem cells are cardioprotective following acute myocardial infarction, Stem Cells Dev. 20 (11) (2011 Nov) 1985–1994, https://doi.org/10.1089/scd.2010.0424.
[50] P.V. Hauser, R. De Fazio, S. Bruno, S. Sdei, C. Grange, B. Bussolati, C. Benedetto, G. Camussi, Stem cells derived from human amniotic fluid contribute to acute kidney injury recovery, Am. J. Pathol. 177 (4) (2010) 2011–2021, https://doi.org/10.2353/ajpath.2010.091245.